Supporting information

Phenothiazine Functionalized Multifunctional A-π-D-π-D-π-A Type Hole Transporting Materials via Sequential C-H Arylation Approach for Efficient and Stable Perovskite Solar Cells

*Chunyuan Lu[†a], Mahalingavelar Paramasivam[†a], Kyutai Park[b], Chul Hoon Kim[b] and Hwan Kyu Kim[*a]*

[a]Global GET-Future Lab, Department of Advanced Materials Chemistry,

Korea University, 2511 Sejong-ro, Sejong 339-700, Korea.

[b]Department of Advanced Materials Chemistry,

Korea University, 2511 Sejong-ro, Sejong 339-700, Korea

†These authors contributed equally to this work.

*To whom correspondence should be addressed: Email: hkk777@korea.ac.kr

Device fabrication

Normal type device with configuration of FTO/compact TiO_2/meso-porous TiO_2/$CH_3NH_3PbI_{3-x}Cl_x$/HTMs/Au was used in this work. The PrSCs were prepared according to the reported method (except for HTMs).[1] In this study, the HTM was subsequently spin-coated onto the perovskite layer at 4000 rpm for *spiro*-**OMeTAD** (3000 rpm for new HTMs solution) for 30 s. 72.3 mg of *spiro*-**OMeTAD** was dissolved in 1 mL chlorobenzene. 17.5 µL of tris(bis(trifluoro-methyl-sulfonyl)imide) (Li-TFSI) stock solution (520 mg mL^{-1} in acetonitrile), 28.8 µL of *tert*-butylpyridine (t-BP) were added to *spiro*-**OMeTAD** solution as additives. New HTMs with concentration (**SGT-421** (25 mg/mL) and **SGT-422** (8mg/mL)) doped by addition of 5.4 µL of Li-TFSI and 9.47 µL of 4-tBP. Finally, 78 nm of Au electrode was deposited by thermal evaporation.

Characterization

The ^{1}H NMR spectra was measured using Varian Mercury 300 spectrometer. The ^{13}C NMR spectra were measured using Bruker Biospin Gmbh AVAVCE II 900 spectrometer. MALDI-TOF mass spectra were recorded by a Voyager-DETM STR biospectrometry workstation. Thermal properties of developed HTMs were analyzed using Sinco DSC N-650 and TGA N-1000. UV/Vis absorption spectra of new HTMs in dichloromethane were measured with Shimadzu UV-2401PC spectrophotometer. Photoluminescence spectra of new HTMs in dichloromethane were analyzed with a Fluorolog FL-3-22 fluorometer from Horiba-Jobin-Yvon Ltd. equipped with a 450 W Xe lamp and two analyzing monochromators. Cyclic voltammetry was measured on a Versa STAT3 (AMETEK). A three-electrode system was used and consisted of a reference electrode (Ag/AgCl), a working electrode (Pt wire), and counter electrode (Pt wire). The redox potentials of HTMs were measured in acetonitrile and tetrahydrofuran with 0.1M TBAPF6 with a scan rate of 50 mV. Current-voltage (I-V) measurements were performed under 100 mW/ cm^2 (AM 1.5G illumination) by a Newport solar simulator and a Keithley model 2400 source meter. The incident photon-to-current efficiency (IPCE) spectra were recorded as a function of wavelength from 300 to 820 nm using a specially designed IPCE system (PV Measurements, Inc.) equiped with a 300W Xenon

lamp (Spectra-Physics). The SEM images were obtained by Hitachi's S-4800 FE-SEM. The AFM images were obtained by AFM using non-contact mode (XE-7 Park Systems). XPS data were obtained by High-performance X-ray Photoelectron Spectrometer (BS101) with an AXIS-NOVA (Kratos) using an Al-Kα X-ray source at 150 W.

Hole mobility measurement

Hole mobility of various HTMs was determined by the space-charge-limited current (SCLC) method,[2-3] which can be described by the following equation:

$$J = \frac{9}{8}\mu\varepsilon_0\varepsilon_r\frac{V^2}{d^3}$$

where *J* is the current density, μ is the hole mobility, ε_o is the vacuum permittivity (8.85×10^{-12} F/ m), ε_r is the dielectric constant of the material (normally taken to approach 3 for organic semiconductors),[4] *V* is the applied bias, and *d* is the film thickness measured through cross-section measurement using field-emission scanning electron microscopy. Device structure: FTO/pedot:pss/HTM/Au was used as hole-only device for SCLC measurement.

Time-resolved photoluminescence

Picosecond time-resolved photoluminescence measurements were made using a commercial picosecond fluorescence lifetime measurement system (Hamamatsu streak camera, C11200). Light source was a commercial optical parametric amplifier (TOPAS-prime, Light-Conversion) seeded with a commercial regenerative amplifier system (Spitfire-Ace, Spectra-Physics) operating at 1 kHz. The center wavelength and pulse energy were adjusted to 500 nm and about 10nJ, respectively. The output was spectrally filtered by using a 500 nm band pass filter. A singlet lens was used to focus the excitation beam to the sample and photoluminescence was collected in a back scattering geometry using a parabolic mirror. The emission was sent to a monochromator and detected with the streak camera. Magic angle detection was used to

avoid the effect of polarization. Widths (FWHM) of the instrumental response were about 2 ns in 500 ns time window. All data were acquired in single photon counting mode using the Hamamatsu U8167 software. All the experiments were carried out at ambient temperature (23^{o}C).

Computational details

Gaussian 09 ab initio quantum chemical software package was used to perform the gas phase DFT calculations.[5] DFT method was employed to obtain the ground-state properties. The global minima on potential energy surface were further confirmed by vibration analysis with zero imaginary frequencies. Structural optimizations were executed without any symmetry constraints in gas phase. The gas phase relaxations of atomic positions was performed by employing the hybrid Becke, three-parameter, Lee-Yang Parr exchange-correlation functional (B3LYP) and 6-311G (d, p) basis set which is extensively used for the ground state calculations in this study.[6-7] The resulted optimized geometries were further used as input to obtain frontier molecular orbitals (FMOs). The geometry optimization of all cations were performed under the UB3LYP/6-31G(d, p) level for all the HTMs.[8]

Materials and Synthesis

Unless otherwise specified, all reactions have been carried out under nitrogen atmosphere with standard Schlenk techniques. All reagents purchased from commercial sources are reagent/ analytical grade and used received without further purification. Sodium and benzophenone were used to distill the solvents under nitrogen atmosphere. All chromatographic separations were carried out on silica gel (100−200 mesh). Solvents were distilled from appropriate reagents.

Synthetic procedures

5-(7-Bromo-10-dodecyl-10H-phenothiazin-3-yl)thiophene-2-carbaldehyde (1)

3,7-dibromo-10-dodecyl-10H-phenothiazine (1.0 eq, 9.52 mmol, 5 g), Cs_2CO_3 (1.5 eq, 14.28 mmol, 4.65 g) and pivalic acid (0.3 eq, 2.86 mmol, 0.29 g) were taken in round bottomed flask with continuously purging of argon. $Pd(OAc)_2$ (3 mol%, 0.29 mmol, 60 mg), JohnPhos ligand (6 mol%, 0.57 mmol, 170 mg) and 2-thiophenecarboxaldehyde (1 equiv, 9.52 mmol, 0.8 g) were added to the reaction flask. 50 mL of toluene was added and the reaction solution was heated at 100 ˚C with vigorous stirring for 20 h. The reaction solution was then cooled to room temperature and filtered through celite pad to remove the inorganic impurities. The filtrate was extracted with CH_2Cl_2. The combined organic layer was washed with water then brine solution and dried over $MgSO_4$, filtered, and evaporated under reduced pressure. The residue was purified through column chromatography over silica gel using Hexane: ethyl acetate (95:5, v/v) as eluent to give the desired product as orange solid (5.4 g, 9.73 mmol, 86%). ^{1}H NMR (300 MHz, Chloroform-d) δ 9.85 (s, 1H), 7.69 (d, J = 4.0 Hz, 1H), 7.43 (dd, J = 8.5, 2.0 Hz, 1H), 7.37 (d, J = 1.9 Hz, 1H), 7.29 – 7.24 (m, 2H), 7.22 (s, 2H), 6.83 (d, J = 8.6 Hz, 1H), 6.69 (d, J = 8.0 Hz, 1H), 3.80 (t, 2H), 1.77 (t, 2H), 1.42 (d, 2H), 1.24 (s, 16H), 0.87 (t, 3H). MS (Maldi-TOF): (m/z) calcd: 555.1265; found: 557.2843.

5,5'-(thiophene-2,5-diylbis(10-dodecyl-10H-phenothiazine-7,3-diyl))bis(thiophene-2-carbaldehyde) (2)

5-(7-Bromo-10-dodecyl-10H-phenothiazin-3-yl)thiophene-2-carbaldehyde (2.2 equiv, 9.15 mmol, 5.09 g), Cs_2CO_3 (2.5 equiv, 10.4 mmol, 3.39 g), $Pd(OAc)_2$ (5 mol %, 0.21 mmol, 0.05 g), JohnPhos (10 mol %, 0.42 mmol, 0.12 g), pivalic acid (60 mol %, 1.25 mmol, 0.26 g) were dissolved in N,N-dimethyl acetamide in round bottomed flask under argon atmosphere. Thiophene (1 equiv, 4.16 mmol, 0.35 g) was added to the reaction mixture and the flask was purged with argon for 15 mins. The reaction mixture was then heated to 100 ˚C with vigorous stirring for 24 h. The reaction solution was then cooled to room temperature and filtered through celite pad to remove the inorganic impurities from the reaction mixture.

Then the filtrate was diluted and extracted with CH_2Cl_2. The combined organic layers were washed several times with water and finally with brine solution. The organic extracts were dried over $MgSO_4$, filtered, and evaporated under reduced pressure. The crude product was purified by column chromatography silica gel over silica gel using *n*-hexane/ CH_2Cl_2/EA (6.5/3/0.5, v/v) to afford the dialdehyde derivative as red solid. Albeit, the dialdehyde derivative has good solubility in CH_2Cl_2, it has an extensive contact with silica gel during column chromatography. Thus, it is necessary to use the proper eluent compositions to obtain the product with good yield. (3.6 g, 3.48 mmol, 76%). ^{1}H NMR (300 MHz, Chloroform-d) δ 9.85 (s, 2H), 7.69 (d, J = 3.9 Hz, 2H), 7.48 – 7.37 (m, 5H), 7.37 – 7.31 (m, 3H), 7.31 – 7.23 (m, 3H), 7.14 (s, 2H), 6.83 (d, J = 8.4 Hz, 4H), 3.84 (t, J = 6.7 Hz, 4H), 1.89 – 1.72 (m, 4H), 1.43 (s, 5H), 1.24 (s, 38H), 0.87 (t, J = 6.5 Hz, 7H). MS (Maldi-TOF): (m/z) calcd: 1034.4041; found: 1034.5138.

5,5'-(((Thiophene-2,5-diylbis(10-dodecyl-10H-phenothiazine-7,3-diyl))bis(thiophene-5,2-diyl)) bis(methanylylidene)) bis(3-methyl-2-thioxothiazolidin-4-one) (SGT-420):

Dialdehyde derivative (1 equiv, 0.6 g, 0.58 mmol) , 3-methyl rhodanine (6 equiv, 0.5 g, 3.5 mmol) and ammonium acetate (20 equiv, 0.89 g, 11.6 mmol) were dissolved in dichloroethane (20 mL) and degassed the reaction solution for 10 minutes. The reaction mixture was heated to reflux with stirring at 80˚C at room temperature for 12 h. The reaction solution was then cooled to room temperature and extracted with CH_2Cl_2. The combined organic layers were washed several times with water and finally with brine solution. The organic extracts were dried over $MgSO_4$, filtered, and evaporated under reduced pressure. Then, solvent was removed in vacuo and the crude product was purified by column chromatography over silica gel using *n*-hexane : CH_2Cl_2, (2:3; v/v) as eluent . The obtained product was recrystallized from chloroform and hexane to afford the desired product as dark brownish red crystals (600 mg, 0.464 mmol, 80%). ^{1}H NMR (300 MHz, Chloroform-*d*) δ 7.86 (s, 2H), 7.38 (dd, *J* = 10.2, 11H), 7.29 (s, 3H), 7.16 (s, 1H), 6.85 (d, *J* = 8.4 Hz, 3H), 3.87 (t, *J* = 6.8 Hz, 4H), 3.52 (s, 6H), 1.87 – 1.78 (m, 4H), 1.48 – 1.41 (m, 4H), 1.25 (s, 32H), 0.87 (t, *J* = 6.1 Hz, 6H). MS (Maldi-TOF): (m/z) calcd: 1292.3455; found: 1292.6186.

2,2'-(((Thiophene-2,5-diylbis(10-dodecyl-10H-phenothiazine-7,3-diyl))bis(thiophene-5,2-diyl))bis(methanylylidene)) dimalononitrile (SGT-421):

This was synthesized by a procedure similar to that of **SGT-420,** except that malononitrile was used instead of 3-methyl rhodanine. The column chromatography was carried out using the following eleuent compositions in the order (Hexane/EA (5:1), Hexane/ CH_2Cl_2 (2:3), CH_2Cl_2 and finally CH_2Cl_2/CH_3OH (95:5)). The obtained product was recrystallized from chloroform and hexane to afford the desired product as black solid. (545 mg, 0.48 mmol, 83%) ^{1}H NMR (300 MHz, Chloroform-*d*) δ 7.75 (s, 2H), 7.67 (d, *J* = 3.9 Hz, 2H), 7.52 – 7.44 (m, 2H), 7.42 (d, *J* = 2.2 Hz, 2H), 7.39 – 7.30 (m, 4H), 7.26 (s, 3H), 6.86 (d, *J* = 8.6 Hz, 4H), 3.87 (t, *J* = 7.1 Hz, 4H), 1.83 (t, 4H), 1.45 (m, 4H), 1.25 (s, 32H), 0.87 (t, *J* = 6.1 Hz, 6H). MS (Maldi-TOF): (m/z) calcd: 1130.4265; found: 1130.3474.

2,2'-(((Thiophene-2,5-diylbis(10-dodecyl-10H-phenothiazine-7,3-diyl))bis(thiophene-5,2-diyl))bis(methanylylidene)) bis(1H-indene-1,3(2H)-dione) (SGT-422):

Dialdehyde derivative (1 equiv, 0.6 g, 0.58 mmol) , 1,3-indanedione (10 equiv, 0.23 g, 3.5 mmol) were dissolved in dry chloroform (50 ml). Triethylamine (0.2 ml) was added dropwise to the reaction solution and the mixture refluxed with stirring at room temperature under nitrogen for 24h. The reaction mixture was quenched with water and extracted with chloroform. The organic extracts were washed with water, brine, and dried over anhydrous magnesium sulfate. The solvent was removed by rotary evaporation, and the residue was purified by column chromatography over silica gel with the following eluent compositions which are given in the order (Hexane/EA (5:1), Hexane/ CH_2Cl_2 (1:4), CH_2Cl_2 and finally CH_2Cl_2/CH_3OH (95:5)). The obtained product was recrystallized from CH_2Cl_2 and acetone (5:20; v/v) to afford the desired product as black solid. (678 mg, 0.525 mmol, 91%)^{1}H NMR (300 MHz, Chloroform-*d*) δ 7.93 (s, 8H), 7.77 (s, 4H), 7.58 – 7.48 (m, 4H), 7.37 (d, *J* = 10.7 Hz, 6H), 7.26 (s, 2H), 7.16 (s, 1H), 6.84 (d, *J* = 7.4 Hz, 3H), 3.87 (s, 4H), 1.82 (q, *J* = 7.4 Hz, 4H), 1.46 (s, 4H), 1.25 (s, 32H), 0.86 (t, *J* = 6.2 Hz, 6H). MS (Maldi-TOF): (m/z) calcd: 1290.4565; found: 1290.8264.

Cost evaluation

To compare the synthesis cost of **SGT-421** with *spiro*-**OMeTAD**, the lab synthesis cost of **SGT-421** was estimated by using the model proposed by Osedach et al.[9] Required amounts of reactants, catalysts, reagents, solvents and materials for workup and purification of the 1 g of **SGT-421** is summarized in **Table S3**. The price of the commercially available chemicals per kg and the cost of the intermediate products per kg were multiplied by the required quantities for the synthesis.

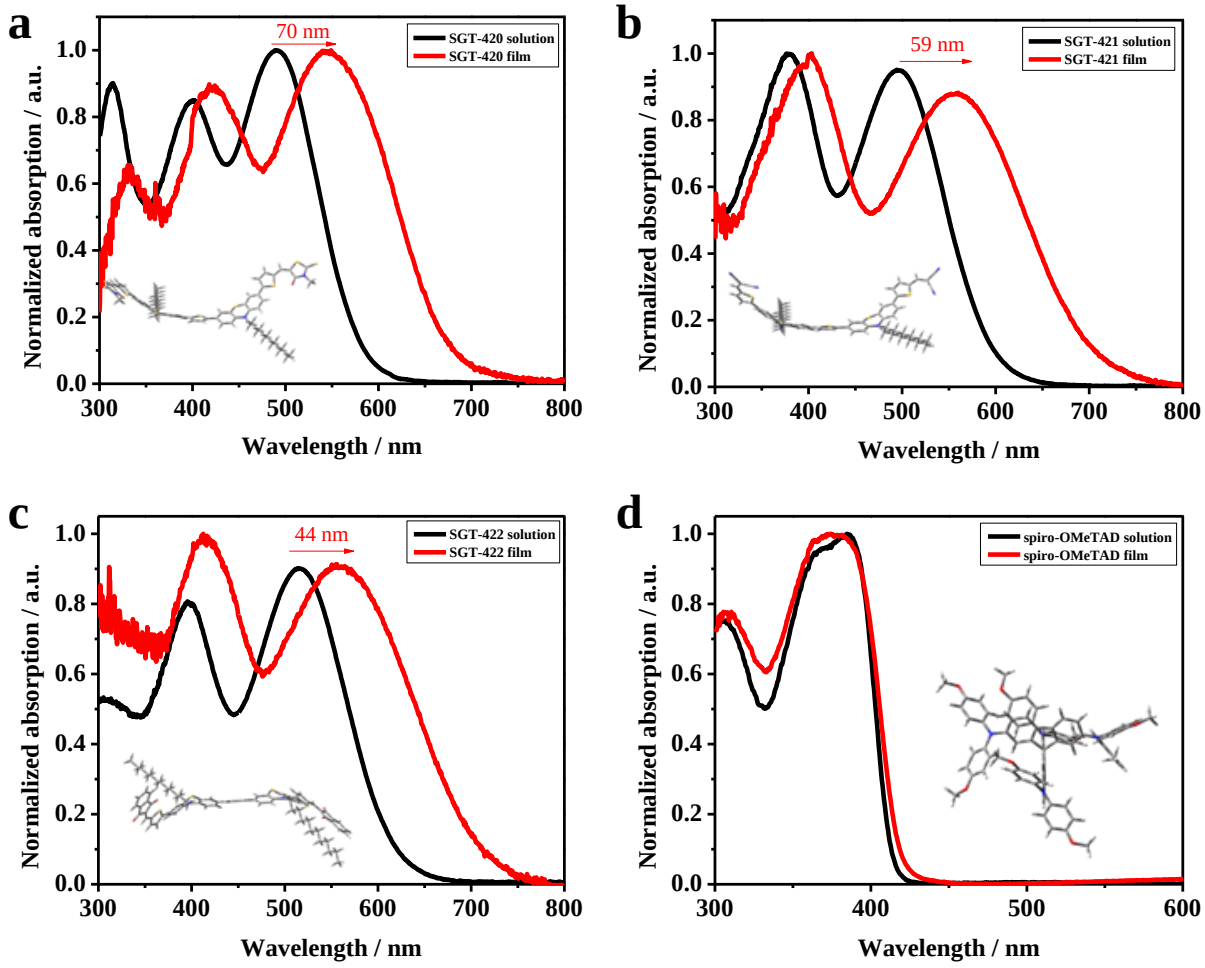

Fig. S1. UV-vis absorption spectra of synthesized HTMs a) **SGT-420**; b) **SGT-421**; c) **SGT-422**; d) *spiro*-**OMeTAD** in CH_2Cl_2 and thin film state;. Inset depicts the corresponding side views of optimized structures of the HTMs obtained from DFT/B3LYP/6-311G (d, p) level of theory.

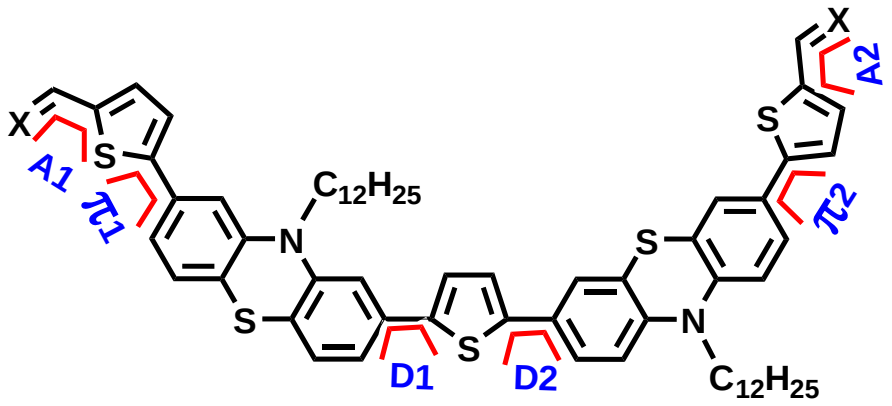

Torsion angles of geometries optimized in ground state (units in degree)

	A1	π1	D1	D2	π2	A2
SGT-420	0.21	-23.19	23.58	24.42	22.23	-0.59
SGT-421	-0.76	20.18	19.78	19.83	20.41	-1.00
SGT-422	-0.35	22.04	23.53	23.14	22.67	-0.63

Fig. S2. Empirical molecular structure for the representation of dihedral angles in the HTMs.

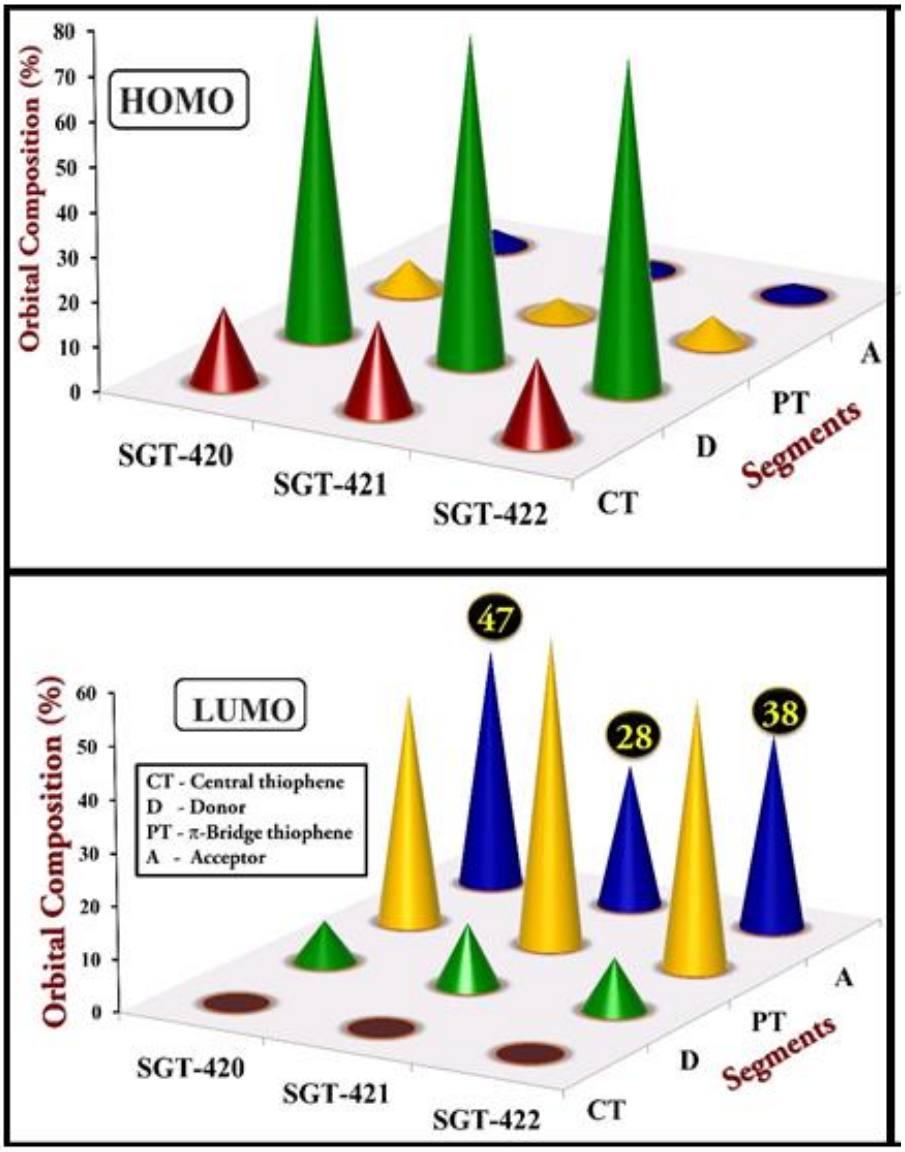

Fig. S3. Percentage contributions of the molecular orbital density from the individual segments in HOMO and LUMO energy levels of the HTMs.

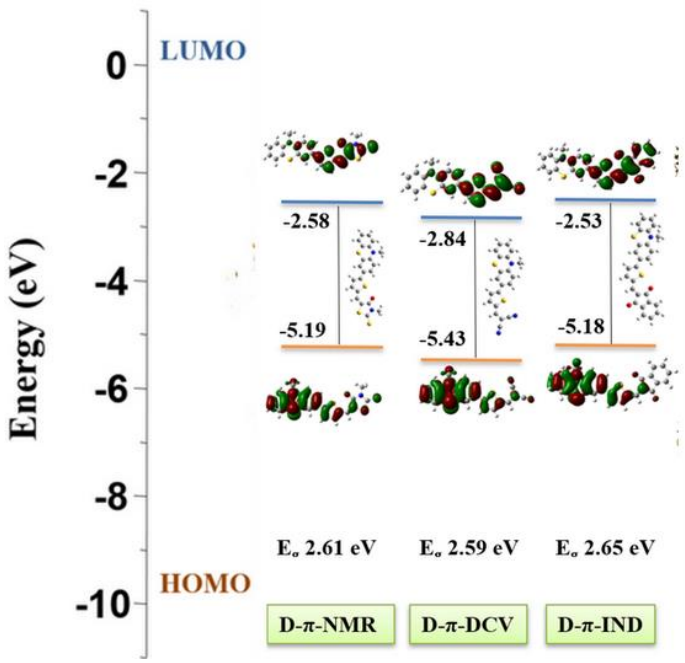

Fig. S4. The isodensity surfaces and energy levels of the model molecules based on D-π-A configuration obtained from DFT/B3LYP/6-311G (d, p) level of theory to ensure the influence of end-capped acceptor units on the energy level regulations in the HTMs.

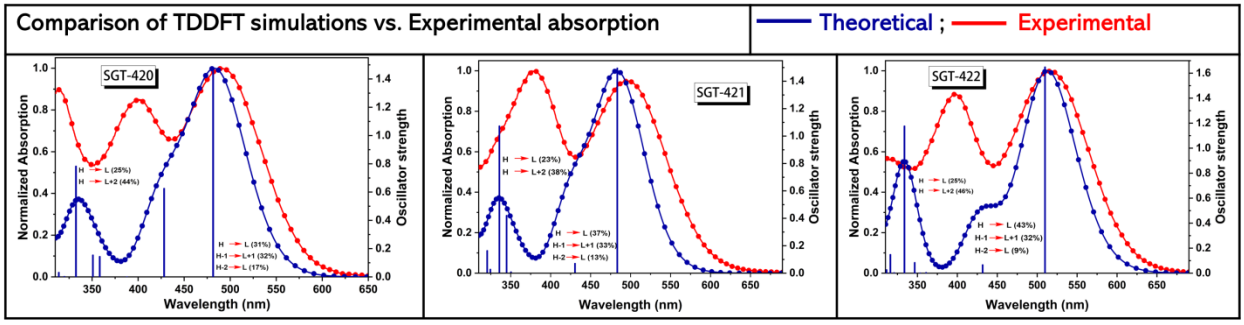

Fig. S5. Simulated absorption spectra obtained with major transitions involved by using the TD-DFT/M06-2X/6-311G (d, p) level of theory in CH_2Cl_2 solvent medium.

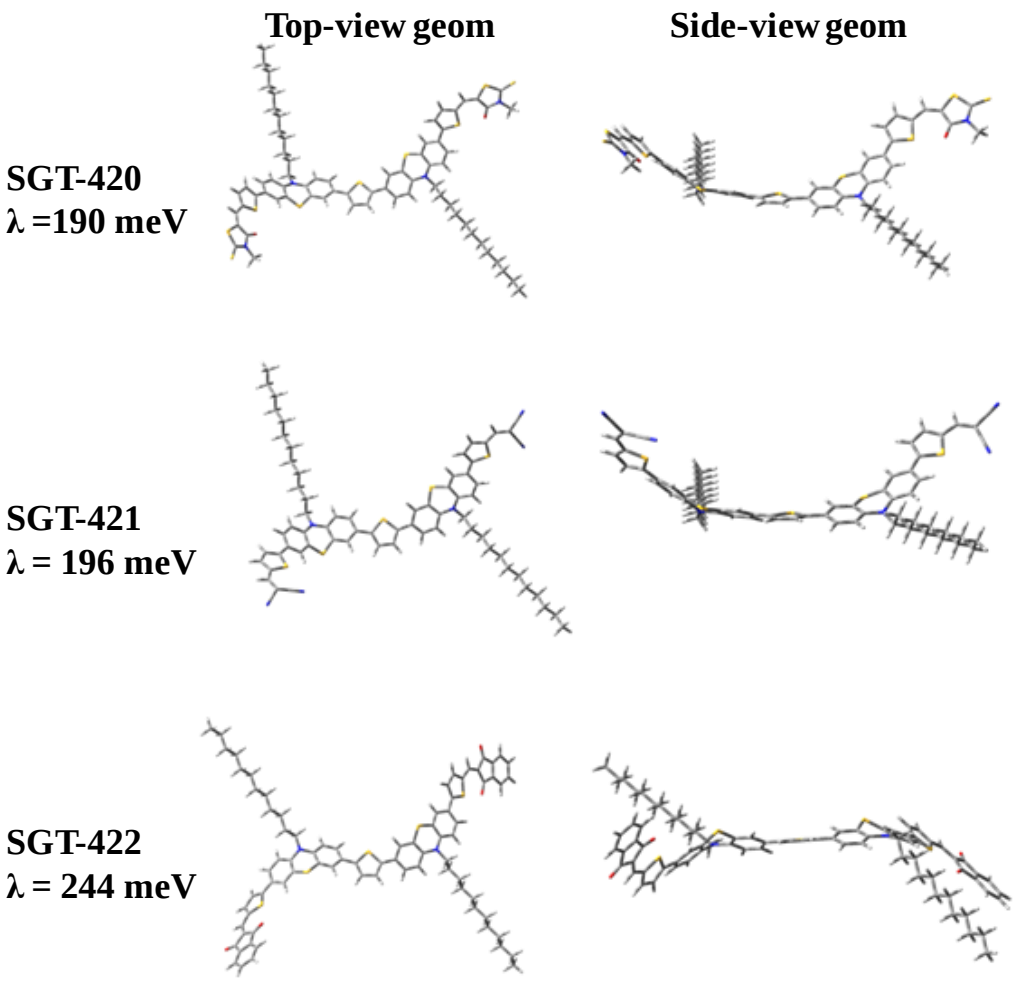

Fig. S6. Top and side view optimized geometry of various HTMs and hole reorganisation energy (λ_h)) of **SGT-420, SGT-421** and **SGT-422.**

Chemical structures of the investigated HTMs

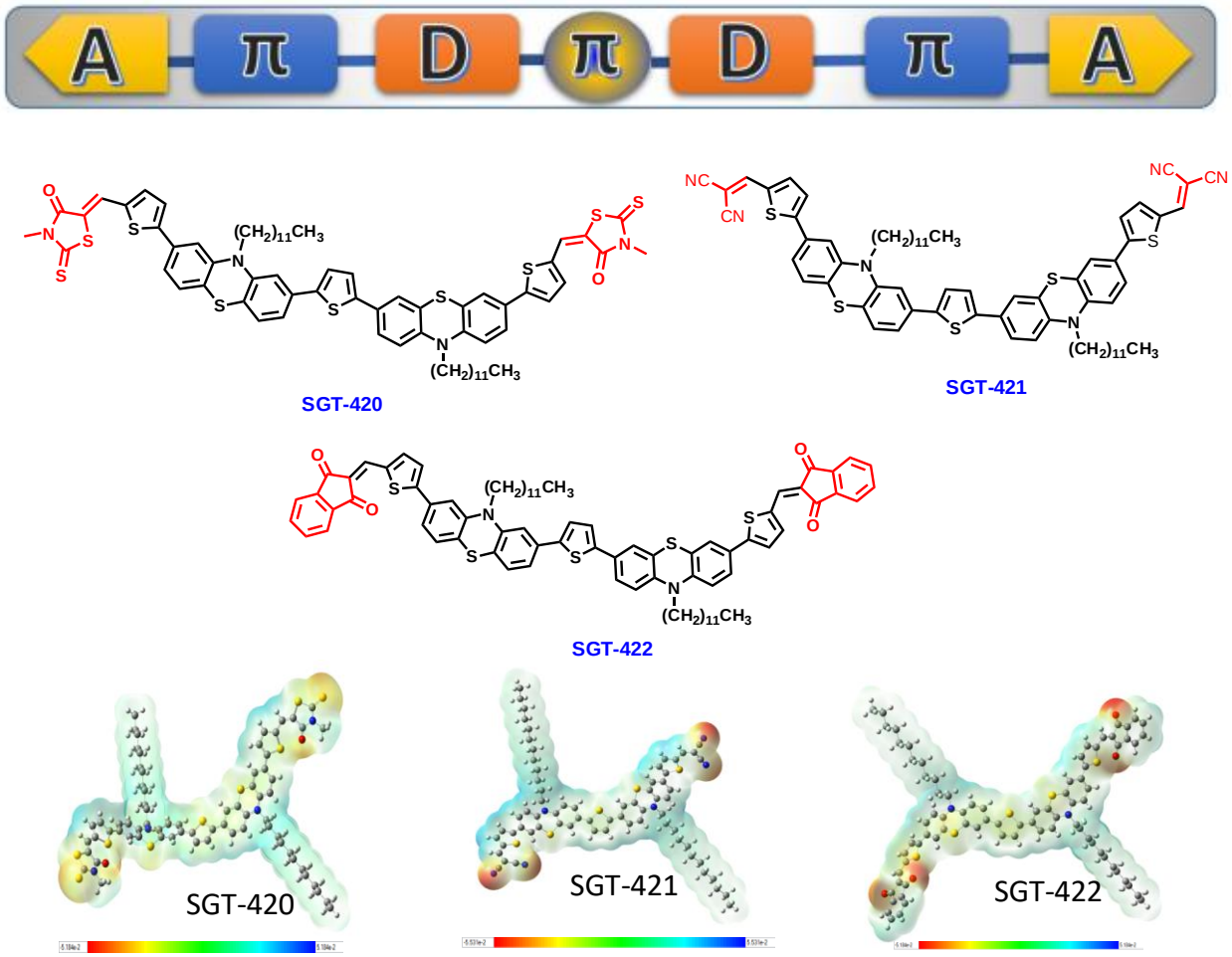

Fig. S7. Chemical structures and electrostatic potential (ESP) surfaces of different HTMs (red colour and blue colour act as regions of negative charge and positive charge, respectively).

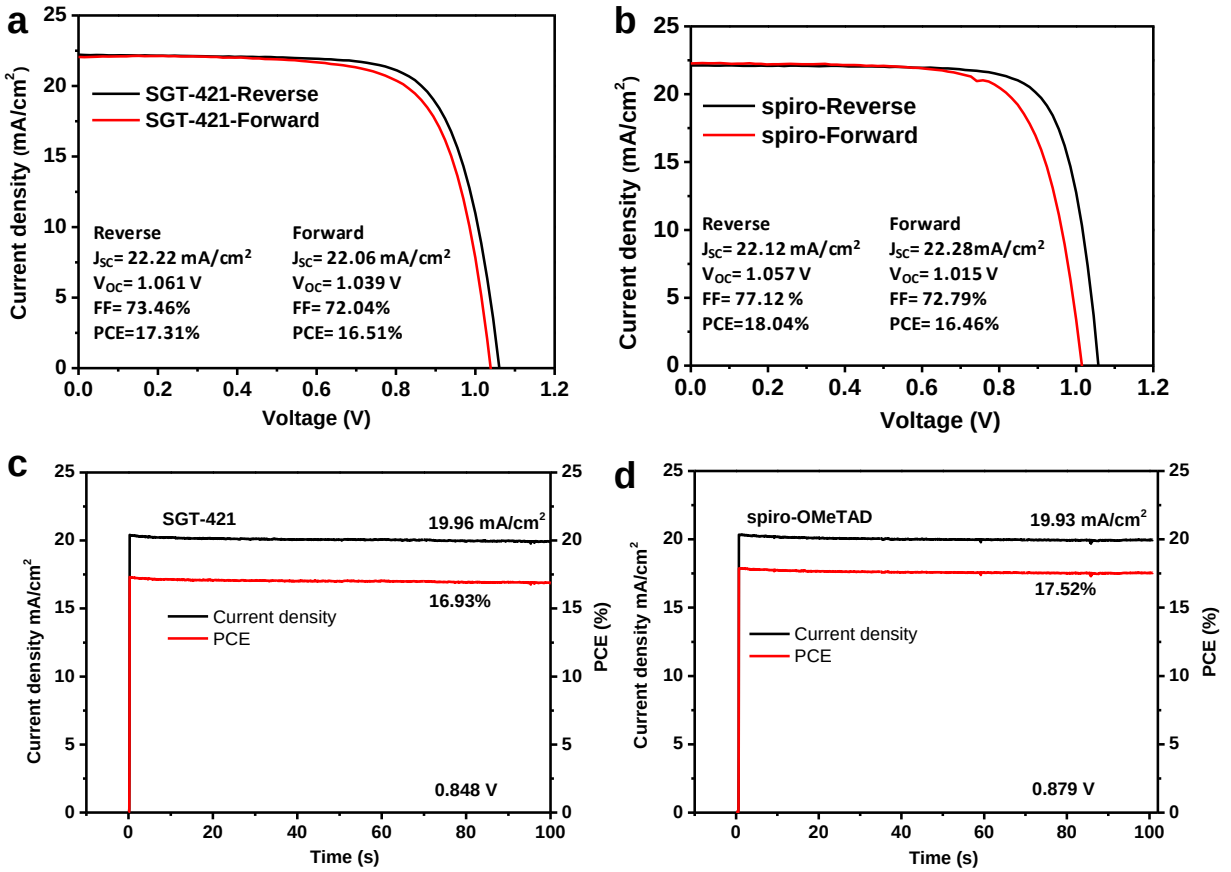

Fig. S8. a-b) J-V curves of perovskite solar cells based on different HTMs under reverse and forward scan. a) **SGT-421** based device; b) spiro-OMeTAD based device; c-d) Stabilized photocurrent density (black color) and power conversion efficiency (red color) obtained while holding the solar cell at 0.848V and 0.879V for **SGT-421** and *spiro*-OMeTAD based devices, respectively.

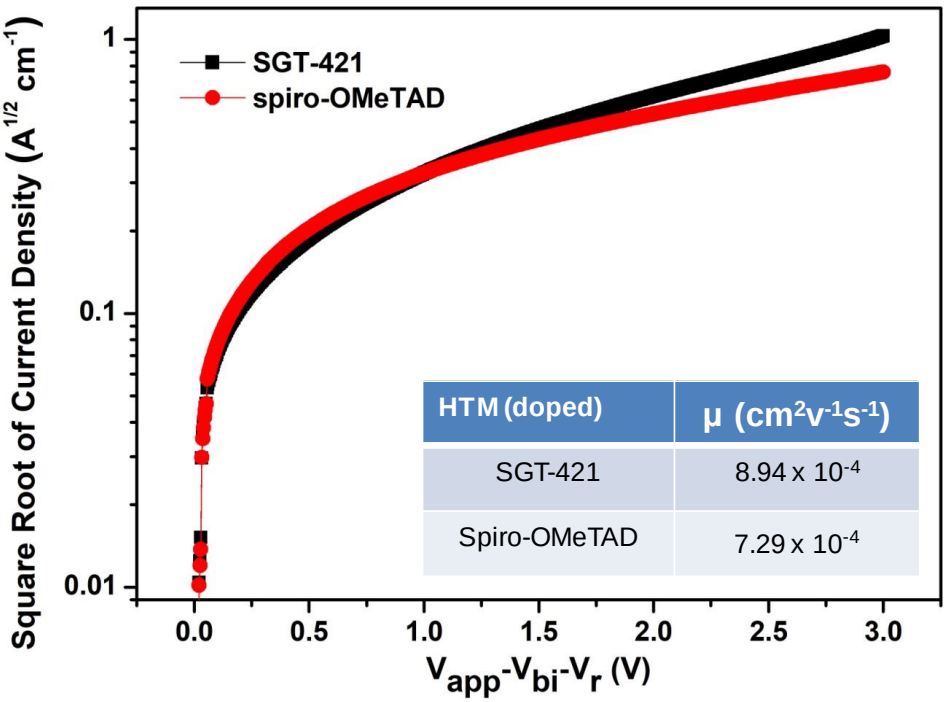

Fig. S9. *J–V* characteristics of doped HTMs in hole-only devices.

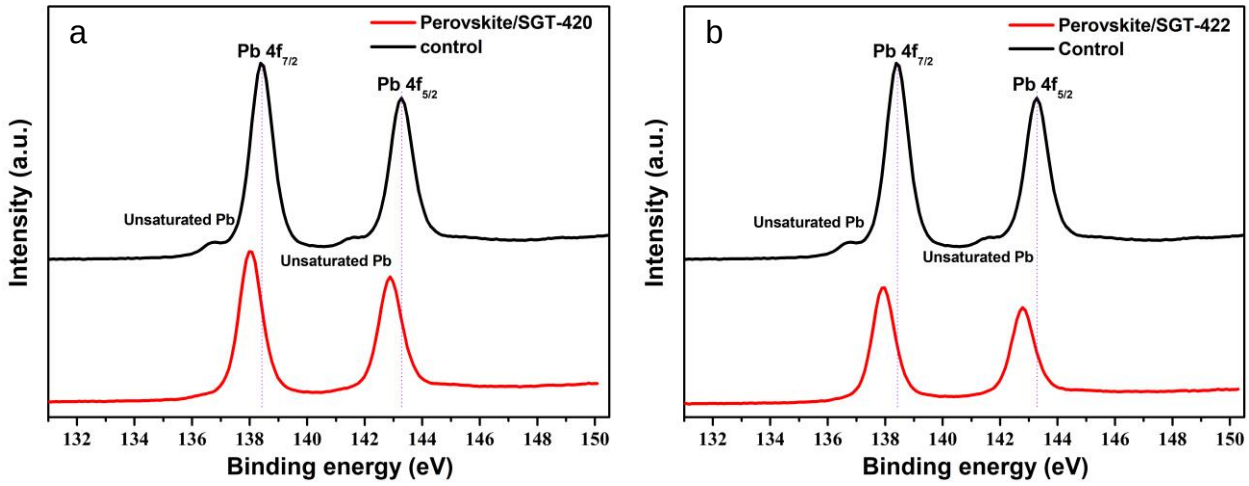

Fig. S10 XPS spectra of Pb atoms in control and passivated perovskite films. a) Perovskite/SGT-420 and control; b) Perovskite/SGT-422 and control.

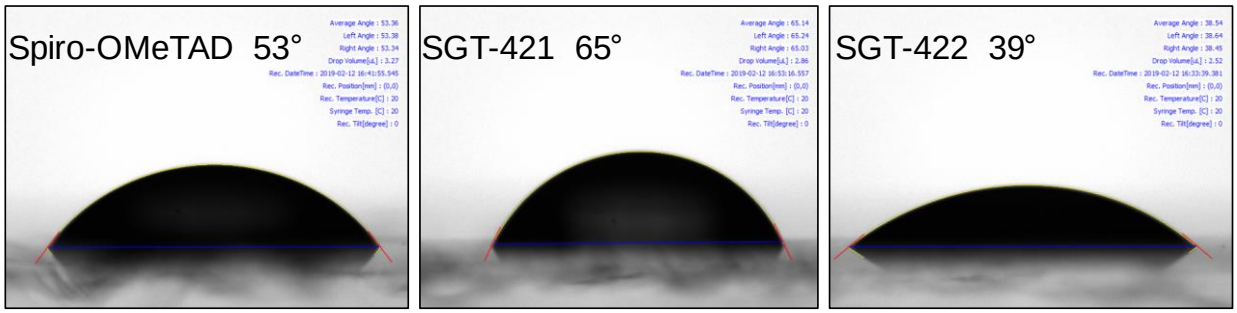

Fig. S11 Water contact angles of various doped HTM films spin-coated on glass.

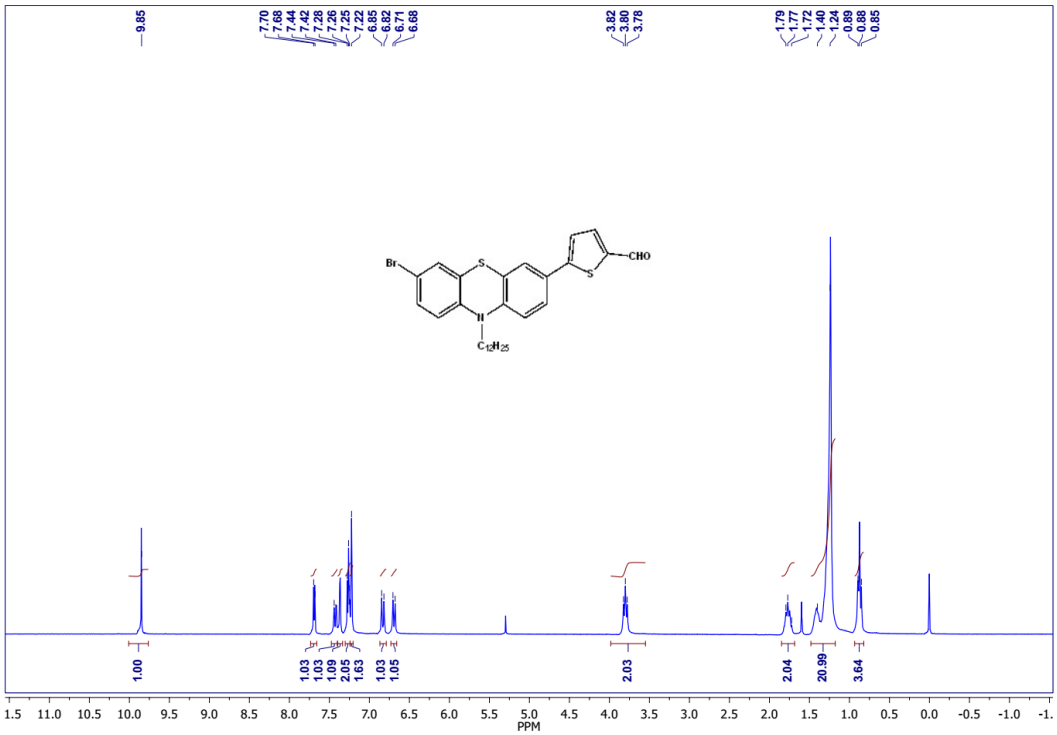

Figure S12. ^{1}H NMR spectrum of compound **1**in $CDCl_3$.

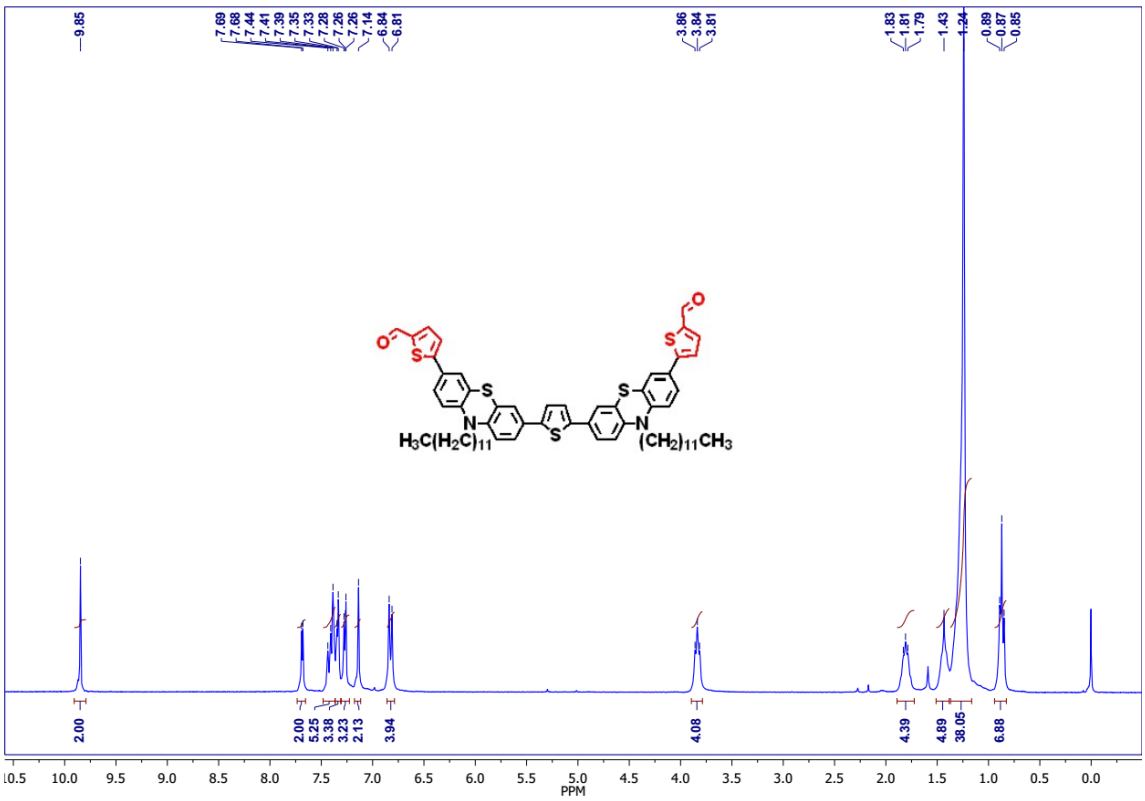

Figure S13. ^{1}H NMR spectrum of compound **2**in $CDCl_3$.

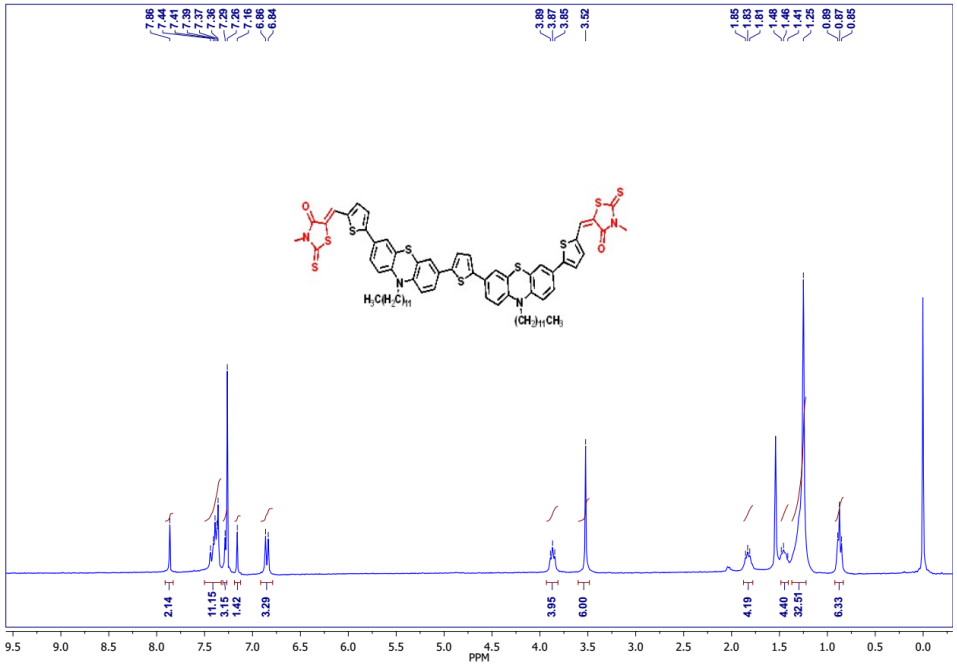

Figure S14. ^{1}H NMR spectrum of compound **SGT-420** in $CDCl_3$.

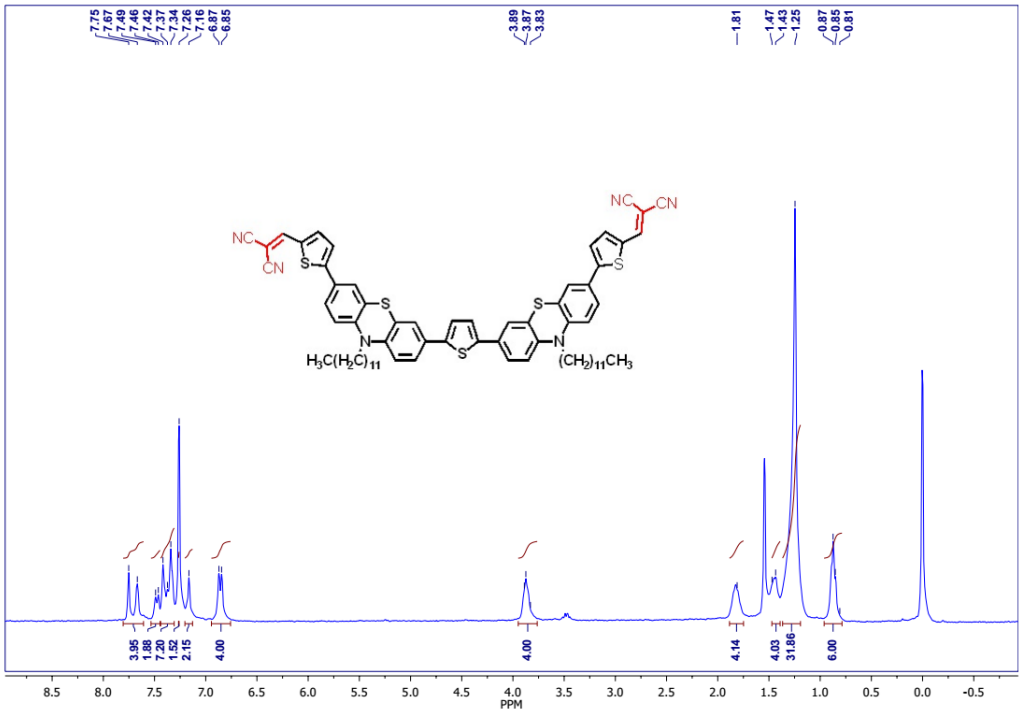

Figure S15. ^{1}H NMR spectrum of compound **SGT-421**in $CDCl_3$.

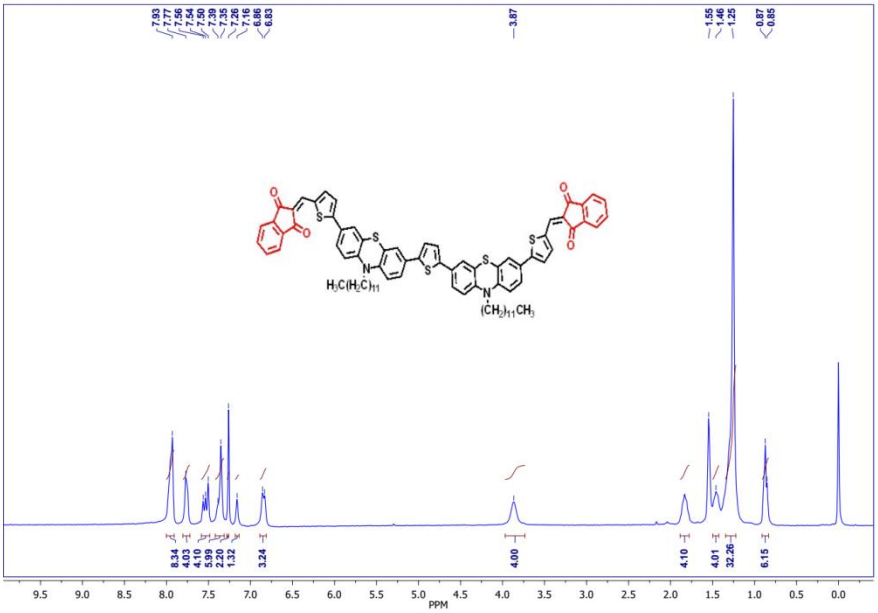

Figure S16. ^{1}H NMR spectrum of compound **SGT-422**in $CDCl_3$.

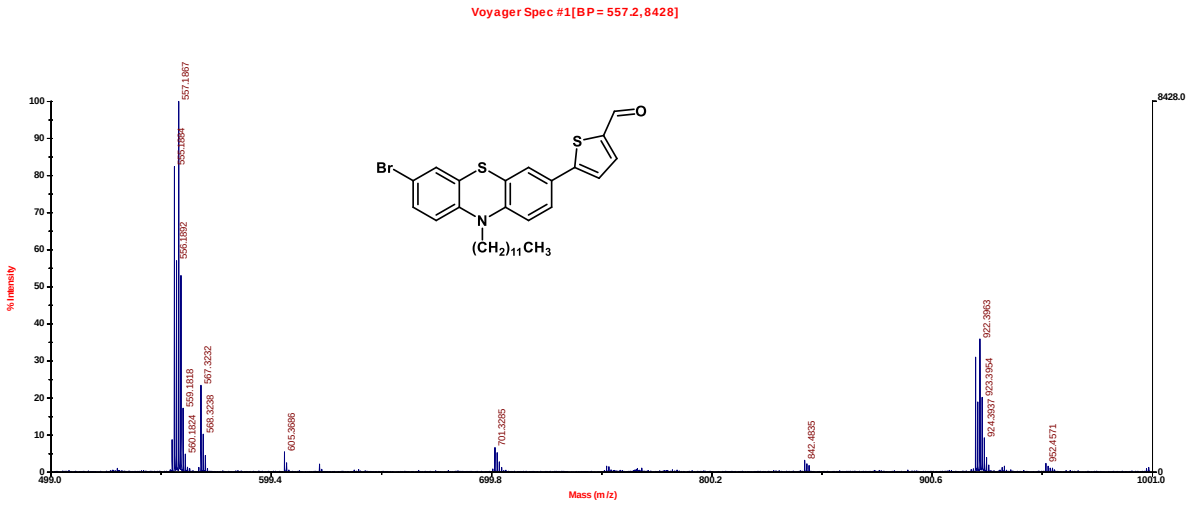

Figure S17. MALDI-TOF spectrum of compound **1.**

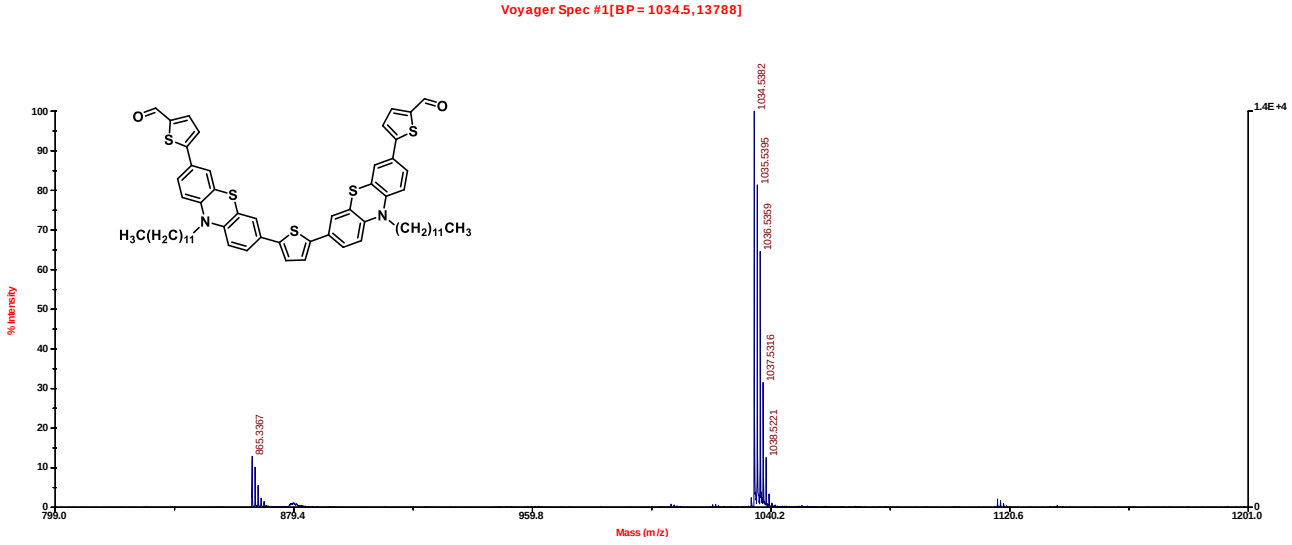

Figure S18. MALDI-TOF spectrum of compound **2.**

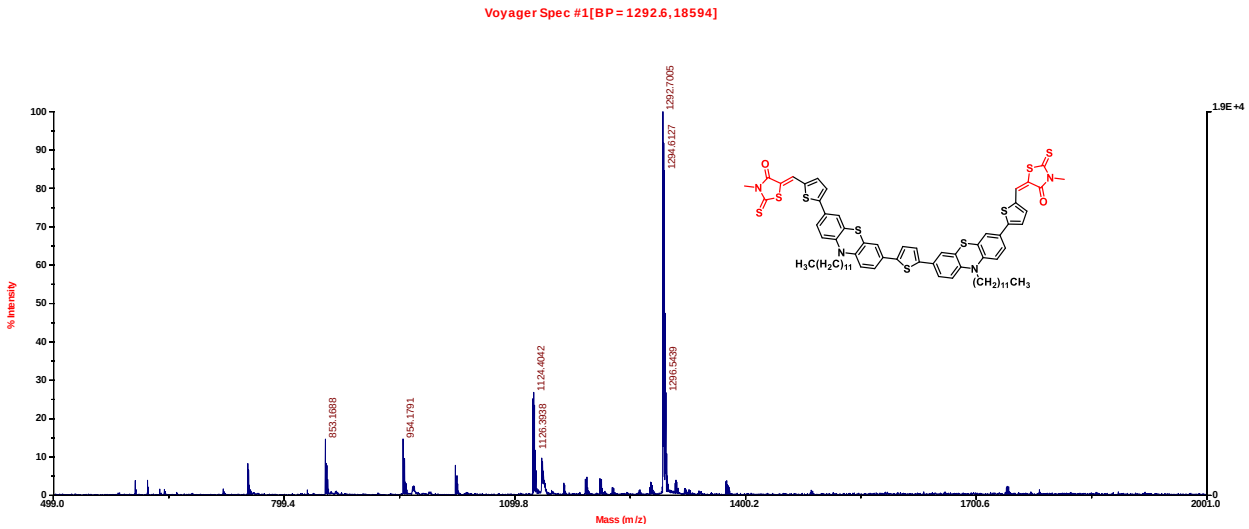

Figure S19. MALDI-TOF spectrum of compound **SGT-420.**

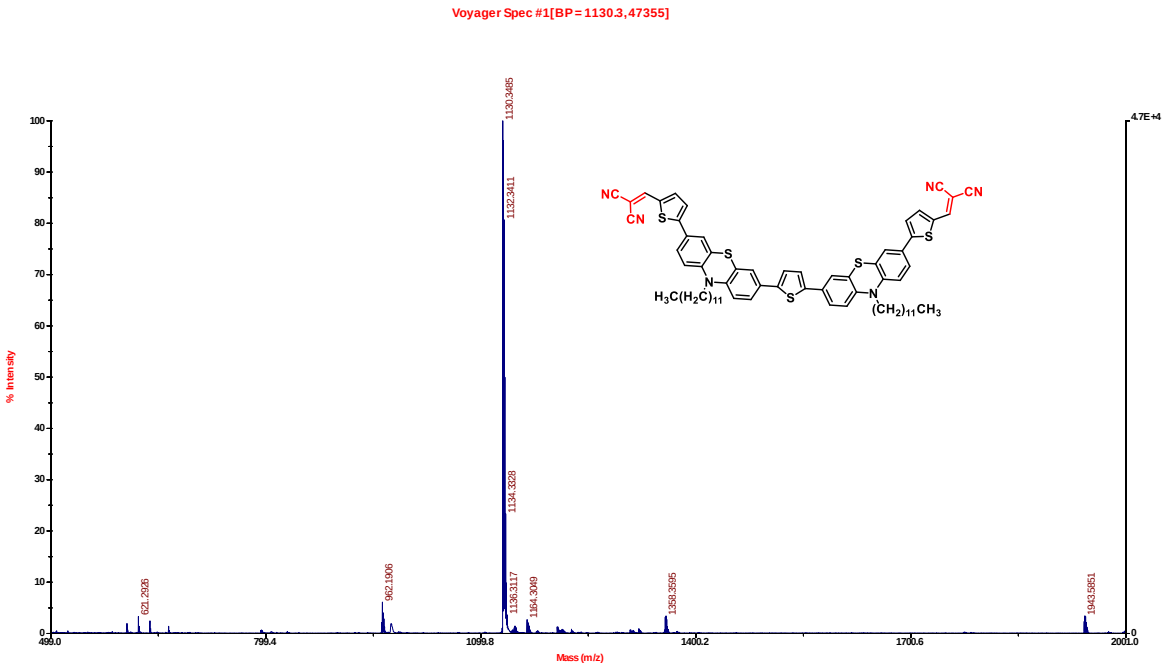

Figure S20. MALDI-TOF spectrum of compound **SGT-421.**

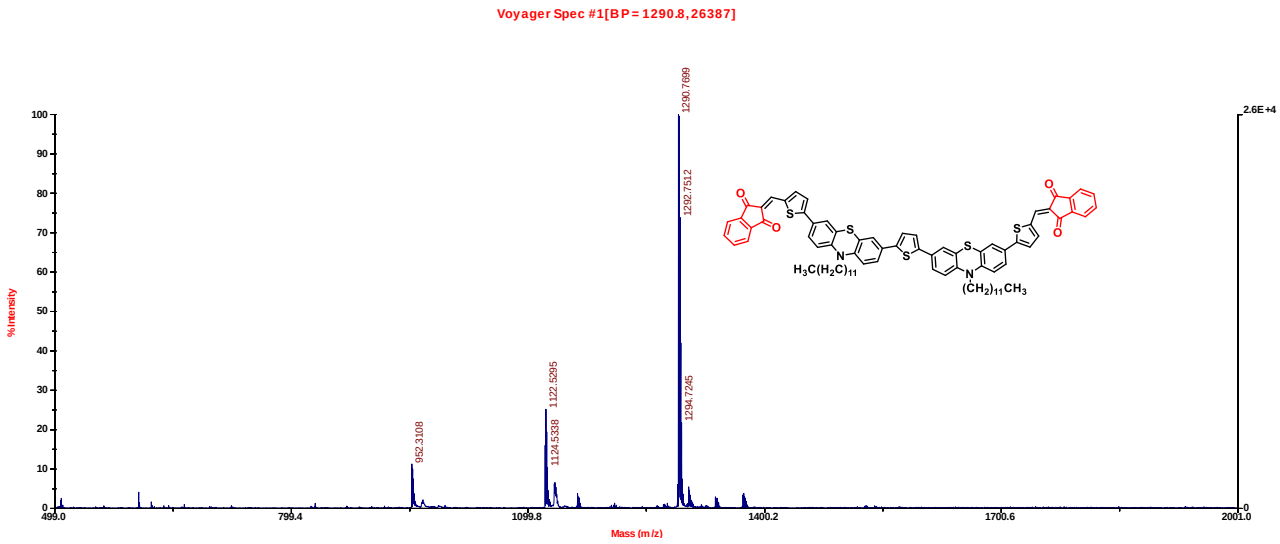

Figure S21. MALDI-TOF spectrum of compound **SGT-422.**

Table S1 Theoretical data of the HTMs.

HTMs	λ_{max}[a] (nm)	M06-2X (CH_2Cl_2) λ_{max} (nm)	Oscillator Strength f	Composition	μ_g[b] (debye)	μ_e[c] (debye)
SGT-420	496 380	481 (2.58 eV)	1.61	H->L (31%) H-1->L+1 (32%) H-2->L (17%)	22.83	28.36
SGT-421	490 398	483 (2.57 eV)	1.53	H->L (37%) H-1->L+1 (33%) H-2->L (13%)	14.76	26.67
SGT-422	516 398	501 (2.47 eV)	1.57	H->L (43%) H-1->L+1 (32%)	9.21	15.84

[a]Experimental absorption values measured in CH_2Cl_2; [b]ground state dipole moment of the HTMs obtained from B3LYP/6-311G(d, p) level of theory; [c]excited state dipole moment of the HTMs.

Table S2. Thermal properties of new developed HTMs and *spiro*-**OMeTAD**.

HTMs	T_g (°C)[a)]	T_m (°C)[b)]	T_{dec} (°C)[c)]
SGT-420	84	209	375
SGT-421	-	-	381
SGT-422	135	-	333
spiro-OMeTAD	126	247	417

[a]glass transition temperature (T_g); [b]melting point (T_m); [c]decomposition temperature (T_{dec}) (corresponding to 5% weight loss);

Table S3. Materials, quantities and cost for the synthesis of **SGT-421**

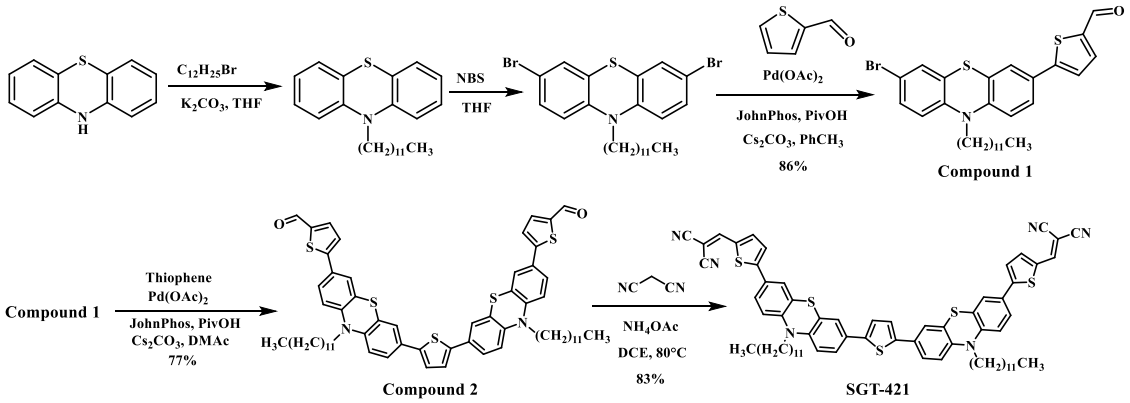

Chemical	Weight reagent (g/g)	Weight solvent (g/g)	Weight workup (g/g)	Price of Chemical (€ /kg)	Chemical Cost (€ /g product)	Cost per step (€ /step)
N-dodecyl phenothizaine						
Phenothiazine	0.35			71.4	0.025	
1-dodecyl bromide	0.58			74.5	0.0432	
K_2CO_3	0.59			56	0.033	
THF		8		8.12	0.984	
Water			20			
Dichloromethane			50	1.42	0.071	
n-hexane			150	3.44	0.516	
$MgSO_4$			2	48.04	0.0961	
						1.7683
3,7-dibromo-10-dodecyl-10H-phenothiazine						
N-dodecyl phenothiazine	0.5					
N-bromoscuccinimide	0.53			81.60	0.0432	
THF		15		8.12	0.1218	
Water			30			
Dichloromethane			50	1.42	0.071	
n-hexane		22.4	300	3.44	1.032	
$MgSO_4$			2	48.04	0.0961	
Silicagel			380	21.19	8.052	
						9.416
5-(7-bromo-10-dodecyl-10H-phenothiazin-3-yl)thiophene-2-carbaldehyde						
3,7-dibromo-10-dodecyl-10H-phenothiazine	0.93					
2-Thiophene carboxaldehyde	0.43			140.3	0.0603	
$Pd(OAc)_2$	0.02			27360	0.5472	
2-(Di-tert-butylphosphino)biphenyl	0.06			3104.5	0.1863	
PivOH	0.03			61	0.0018	
Cs_2CO_3	0.62			216.2	0.1340	
Toluene		6		3.61	0.0217	
Water			50			
Dichloromethane			120	1.42	0.1704	
$MgSO_4$			5	48.04	0.2402	
n-hexane			450	3.44	1.548	
Silicagel			350	21.19	7.4165	
						10.326
5,5'-(thiophene-2,5-diylbis(10-dodecyl-10H-phenothiazine-7,3-diyl))bis(thiophene-2-carbaldehyde) (compound						

2)						
Thiophene	0.2			80.9	0.0162	
5-(7-bromo-10-dodecyl-10H-phenothiazin-3-yl)thiophene-2-carbaldehyde	5.09					
$Pd(OAc)_2$	0.05			27360	1.368	
2-(Di-tert-butylphosphino)biphenyl	0.14			3104.5	0.4346	
PivOH	0.15			61	0.0092	
Cs_2CO_3	3.10			216.2	0.6702	
Dimethylacetamide		12		90.7	1.089	
Water			60			
Dichloromethane			300	1.42	0.426	
$MgSO_4$			15	48.04	0.7206	
n-hexane			400	3.44	1.376	
Ethyl acetate			30	2.07	0.0621	
Silicagel			280	21.19	5.9332	
						12.105
SGT-421						
compound 2	1.1					
Malononitrile	0.7			113	0.0791	
NH_4OAc	3.28			33.3	0.1092	
Dichloroethane		25		8.5	0.2125	
Water			100			
Dichloromethane			1500	1.42	2.13	
MgSO4			10	48.04	0.4804	
Ethyl acetate			80	2.07	0.1656	
Methanol			10	1.735	0.0174	
n-hexane			420	3.44	1.4448	
Silica gel			300	21.19	6.357	
						10.996
Total						44.61 €

References:

(1) Lu, C.; Choi, I. T.; Kim, J.; Kim, H. K. Simple Synthesis and Molecular Engineering of Low-Cost and Star-Shaped Carbazole-Based Hole Transporting Materials for Highly Efficient Perovskite Solar Cells. *J. Mater. Chem. A* **2017,** *5*, 20263-20276.

(2) Poplavskyy, D.; Nelson, J. Nondispersive Hole Transport in Amorphous Films of Methoxy-Spirofluorene-Arylamine Organic Compound. *J. Appl. Phys.* **2003,** *93*, 341-346.

(3) Leijtens, T.; Ding, I. K.; Giovenzana, T.; Bloking, J. T.; McGehee, M. D.; Sellinger, A. Hole Transport Materials with Low Glass Transition Temperatures and High Solubility for Application in Solid-State Dye-Sensitized Solar Cells. *ACS Nano* **2012,** *6*, 1455-1462.

(4) Snaith, H. J.; Grätzel, M. Enhanced Charge Mobility in a Molecular Hole Transporter Via Addition of Redox Inactive Ionic Dopant: Implication to Dye-Sensitized Solar Cells. *Appl. Phys. Lett.* **2006,** *89*, 262114.

(5) Frisch, M. J. T., G. W. ; Schlegel, H. B.; Scuseria, G. E.; Robb, M. A. ; Cheeseman, J. R.; Scalmani, G.; Barone, V.; Mennucci, B.; Petersson, G. A.; et al. Gaussian 09, Revision B.01; Gaussian, Inc.:. *Wallingford, CT* **2010**.

(6) Becke, A. D. Density-Functional Thermochemistry. Iii. The Role of Exact Exchange. *J. Chem. Phys.* **1993,** *98*, 5648-5652.

(7) Becke, A. D. Density-Functional Thermochemistry. Iv. A New Dynamical Correlation Functional and Implications for Exact-Exchange Mixing. *J. Chem. Phys.* **1996,** *104*, 1040-1046.

(8) Priyanka, B.; Anusha, V.; Bhanuprakash, K. Toward Designing Efficient Multifunctional Bipolar Molecules: Dft Study of Hole and Electron Mobilities of 1,3,4-Oxadiazole Derivatives. *J. Phys. Chem. C* **2015,** *119*, 12251-12261.

(9) Osedach, T. P.; Andrew, T. L.; Bulovic, V. Effect of Synthetic Accessibility on the Commercial Viability of Organic Photovoltaics. *Energy Environ. Sci.* **2013,** *6*, 711-718.